An anatomical and functional model of the human tracheobronchial tree

M. Florens[1*], B. Sapoval[1, 2], and M. Filoche[1, 2]

1. CMLA, ENS Cachan, CNRS, UniverSud, 61 Avenue du Président Wilson, F-94230 Cachan, France

2. Physique de la Matière Condensée, CNRS, Ecole Polytechnique, 91128 Palaiseau, France

* Corresponding author: magali.florens@cmla.ens-cachan.fr

Abstract

The human tracheobronchial tree is a complex branched distribution system in charge of renewing the air inside the acini which are the gas exchange units. We present here a systematic geometrical model of this system described as a self-similar assembly of rigid pipes. It includes the specific geometry of the upper bronchial tree and a self-similar intermediary tree with a systematic branching asymmetry. It ends by the terminal bronchioles whose generations range from 8 to 22. Unlike classical models, it does not rely on a simple scaling law. With a limited number of parameters this model reproduces the morphometric data from various sources (31,6), and the main characteristics of the ventilation. Studying various types of random variations of the airway sizes, we show that strong correlations are needed in order to reproduce the measured distributions. Moreover, the ventilation performances are observed to be robust against anatomical variability. The same methodology applied to the rat also permits to build a geometrical model that reproduces the anatomical and ventilation characteristics of this animal. This simple model can be directly used as a common description of the entire tree in analytical or numerical studies such as the computation of air flow distribution or aerosol transport.

Keywords: lungs; airways; geometry; asymmetry; robustness.

Introduction

The tracheobronchial tree is a branched distribution system that carries air from the trachea down to the acini which are the gas exchange units of the lung. At each generation, the branching is essentially dichotomous, each airway being divided into two smaller daughter airways (31,5). The tree starts at the trachea (generation 0) whose average diameter and length are respectively D_0=1.8 cm and L_0=12 cm in the healthy human adult (22), and ends in the terminal bronchioles. From the trachea to the terminal bronchioles (located on average around generation 15) the airways are purely conducting pipes. Since no gas exchanges take place in this region, the volume is called the *dead space volume* (DSV). At rest, an average volume of 0.5 L of fresh air, called the *tidal volume* (TV), is inspired during an average inspiratory time of 2 seconds. Fresh air first fills the extra-thoracic airways (about 0.11 L) then the DSV (about 0.15 L). Finally, 0.24 L is distributed among all acini if all of them are ventilated with fresh air.

From the point of view of fluid transport, the airways can essentially be modeled as a complex arrangement of about 30,000 cylindrical pipes defined by their diameter and length. A better understanding of such a system through analytical studies or numerical computations thus calls for a simplification and a synthesis of this enormous data quantity.

One of the most famous structural models of the tracheobronchial system is the so-called Weibel's "A" model introduced in 1963 (31). In this model, the tree is likened to a hierarchical network of cylindrical pipes with symmetrical branching. An even simpler version of this model assumes a scaling ratio between the parent and the daughter airway diameters equal to $2^{-1/3} \approx 0.79$. This value corresponds to the Hess-Murray law (4,17) when applied to a symmetrical branching. Although widely used

and studied (11,15), this geometrical model does not reproduce several key features of the bronchial tree: in particular, at a given generation, all bronchi are supposed to have the same diameter which is in contradiction with the anatomical distribution of the airway sizes at a given generation (31) (Fig. 1.A).

Two important features have to be included. First, the airway dimensions in the first generations (0-4) are specific to the human anatomy (6,27,14,20,21,30) and they are essentially independent of physiological variability (14). Second, for higher generations (5-15), a systematic branching asymmetry has been observed in the tree bifurcations (14). In other words, each parent airway gives rise to a larger daughter airway and a smaller daughter airway. This asymmetry was already taken into account in Weibel's "B" model, but without being supported by a mathematical model (31).

In this paper, we introduce a new geometrical model based on a limited set of parameters that permits to account for the basic geometrical properties of the tracheobronchial system. We then use this geometrical model to study the ventilation properties of the lung airway system.

Methods

Anatomical model

The model described here is suggested by the morphometric measurements realized by Raabe et al. (22), later analyzed by Majumdar et al. (14). The key ingredient is to assume a systematic branching asymmetry for all generations: each parent airway gives rise to a larger daughter airway (diameter ratio $h_{0,max}$), called the major airway, and a smaller daughter airway (diameter ratio $h_{0,min}$), called the minor airway (Fig. 2). The diameter ratio $h_{0,max}$ (resp. $h_{0,min}$) is defined by the ratio of the diameter of the major (resp. minor) airway over the diameter of the parent airway.

For the proximal airways, the diameter ratios are specific to the human anatomy (generations 0-4). For the intermediate tree, the diameter ratios are considered to be constant (independent of the generation), a good approximation above generation 4. This creates a self-similar intermediate tree. The branch lengths in first approximation are assumed to be directly proportional to the diameter with a length over diameter ratio *L*/*D* specific for the proximal tree and taken equal to 3 in the intermediate tree (31,33,10). This is an approximation as the measured distribution of *L/D* is spread (22) and the average value of *L/D* starts to decrease above generation 16 in Weibel's "A" model to reach 1.2 at generation 23. However, we will show later in the paper that this assumption does not significantly affect the ventilation properties of the tree.

These scaling properties allow to fully determine the geometry of all airways. For example, the diameter *D* of a given airway at generation *G* is the product of the diameter of the trachea D_0 by all the diameter ratios h_g along the pathway from the trachea to this airway.

$$D = D_0 \left(\prod_{g=1}^{G} h_g \right) \qquad (1)$$

The airway length is deduced from the diameter through the length over diameter ratio L/D defined at generation G.

Last, we need to determine an ending condition for the tree. Morphometric studies report that the terminal bronchioles – those that end the tree – are characterized by an average diameter equal to 0.5 mm (33). If one introduces the systematic asymmetry in Weibel's model of 15 generations, the end diameters range from 0.05 mm (obtained for the pathway following the minor airways exclusively) to 1.93 mm (following the major airways exclusively). This is inconsistent with anatomical observations. To reconcile asymmetry and the size of terminal bronchioles, one has to consider that different pathways may comprise different number of generations. In other words, the end of a pathway has to be determined by the airway diameter (0.5 mm) and not by the generation number. This is the criterion used in our model.

In summary, our model is characterized by three main ingredients:

- a specific description of the diameter ratios in the proximal airways (generations 0 to 4).
- a systematic scaling with branching asymmetry in the intermediate tree (generations 5 to 23).
- a cutoff diameter for all terminal airways.

Table 1 summarizes the full set of parameters used in this geometrical model. We now examine the ventilation model that can be built from this geometrical description.

Ventilation model

We focus in this paper on the inspiration at rest. Inspiration is modeled by a constant air flow rate Φ_0 entering the trachea during a duration t_{ins} of 2 seconds, with an air velocity of v_0 = 1 m/s. This can be considered as a good approximation during the

inspiratory phase (32) as the growth and decrease of the flow at the beginning and end of inspiration are relatively short as compared to the plateau phase.

Each acinus is assumed to act as a hydrodynamic pump draining the same flow rate Φ_{ter}. Then by simple flow conservation, the flow rate Φ_{ter} in any terminal bronchiole is equal to Φ_0/N_{ter}, N_{ter} being the number of acini. In other terms, the gas exchange units are considered to be equitably ventilated (34). Note that an identical volume of gas entering each acinus does not mean an identical quantity of oxygen entering each acinus since the volume of fresh air depends on the airway pathways leading to the different acini.

In this steady-state ventilation model, the flow rate in any airway is equal to $n_{ter}\Phi_{ter}$, n_{ter} being the number of acini downstream of this airway. As a consequence, at a given generation, the larger the airway, the larger the flow in it.

The time τ to cross an airway is directly derived from the flow rate and the branch sizes: it is equal to the airway length L divided by the air velocity v which in turn is equal to the flow rate Φ divided by the airway cross section.

$$\tau = \frac{L}{v} = L\frac{\pi D^2/4}{\Phi} \qquad (2)$$

The transit time t_{tr} of an oxygen molecule from the entrance of the trachea to a given acinus is then simply the sum of all times to cross the airways along the pathway leading to this acinus:

$$t_{tr} = \sum_{g=0}^{G} \tau_g = \sum_{g=0}^{G} L_g \frac{\pi D_g^2}{4\Phi_g} \qquad (3)$$

The oxygenation time t_{ox} in one acinus is defined as the time during which fresh air is delivered to this acinus. It is then obtained by subtracting from the total duration of

inspiration, t_{ins}, the time spent in the oropharyngeal and laryngeal cavity, t_{ext}, plus the transit time specific to each acinus t_{tr}:

$$t_{ox} = t_{ins} - (t_{ext} + t_{tr}) \qquad (4)$$

The time t_{ext} spent in the oropharyngeal and laryngeal cavity is deduced from the flow rate entering the trachea Φ_0 and the volume of this cavity estimated to V_{ext} = 106 mL (18,25).

$$t_{ext} = \frac{V_{ext}}{\Phi_0} = \frac{V_{ext}}{v_0 \pi D_O^2 / 4} \approx 0.4\,s \qquad (5)$$

Note that the time τ can be rewritten in terms of the diameter D and the length over diameter ratio L/D:

$$\tau = \frac{\pi}{4\,\Phi}\left(\frac{L}{D}\right)D^3 \qquad (6)$$

So the time τ to cross an airway linearly depends on L/D, but depends on the third power of the diameter D. As a consequence, variations of the diameter have a much greater impact on the time τ than variations of the L/D ratio. To test that, the L/D ratios in the intermediate tree were randomized according to a Gaussian law of mean 3 and standard deviation 0.5 (similar to the spread distribution measured in (22)). The *DSV* and the average oxygenation time were then computed for a large number of trees. Both quantities were found to be spread around their original value with standard deviations respectively equal to 8% and 5%. In a first approximation, one can then assume that the transit times are not affected by a small variation of the L/D ratio.

In this model, a given acinus receives fresh air only if its oxygenation time is positive which means only if the transit time to reach this acinus is smaller than 1.6 s.

Consequently, the volume of fresh air V_{fresh} delivered to one acinus during inspiration writes:

$$\begin{cases} V_{fresh} = \Phi_{ter} t_{ox} & if\ t_{ox} > 0 \\ V_{fresh} = 0 & if\ t_{ox} \leq 0 \end{cases} \quad (7)$$

Finally, the total volume of fresh air delivered through the tracheobronchial tree is simply the sum of the volumes delivered to each acinus.

We propose then a geometrical model of the tracheobronchial tree and a subsequent computation of oxygen ventilation in the human tree at inspiration. In the following, we will compare the geometrical model with morphometric measurements (31,6,22) and with other models from the literature. We will then examine the ventilation properties. We will end the study of the human bronchial tree by testing the robustness of both models against anatomical and physiological variability. Finally, we will show in a brief section that the exact same approach can be used to describe the bronchial tree of the rat.

Results and Discussions

Anatomical data

The parameters of Table 1 build an asymmetric model of the human tracheobronchial tree of variable depth. Generation numbers of the terminal airways range from 9 to 23 with an average value around 15-16 and a standard deviation of 2. This fits Weibel's data locating the terminal airways around generation 14-15 with a standard deviation of 3-4 (34), and also with Kitaoka's model locating terminal airways around generation 15.9 with a standard deviation of 2 (9). Our model gives an average number of acini around 23,000. A classical estimate of the number of acini is about 30,000 (33,5). However, Beech and coworkers recently estimated the number of acini

between 15,000 and 61,000 (1). The average DSV found in our model is 153 mL, in good agreement with estimations from the literature that range from 150 mL (35) to 170 mL (32).

Fig. 1 compares the distribution of airway sizes in our model with anatomical measurements. Fig. 1.A and 1.C present the distribution of generations for airways of diameter 2 mm (31), while Fig. 1.B and 1.D present the distribution of generations of airways giving rise to daughter branches of diameter smaller than 0.7 mm (6).

In both cases, the distributions of the model fit quite well the anatomical distributions measured by Weibel (Fig. 1.A and 1.C) (31) and also the model and measurements realized by Horsfield (Fig. 1.B and 1.D) (6). Nevertheless, the average generation of the computed distribution on Fig. 1.C is slightly larger than that of the measurements (Fig. 1.A). One has to note that Fig. 1.A is built from the Weibel's cast and Fig. 1.C from the Raabe's casts. The shift between both figures could thus be explained by the different techniques used to cast the lung (7). Moreover, the distribution on Fig. 1.D is obtained using specific values of the diameter ratios and identical cutoff diameters for all terminal airways. This leads to discrete size effects that explain the difference between distributions in Fig. 1.B and Fig. 1.D, particularly in generations 13 to 14. These discrete effects are cancelled by a small randomization of the diameter ratios tested further in the paper and observed in Fig. 6C.

Fig. 3 presents the distributions of airway diameters in generations 1 to 10: these distributions are also in good agreement with the distributions measured by Weibel (31). The distributions of airway lengths in generations 1 to 10 reproduce also quite well the measured distributions by Weibel (31) (results not shown). Again, it has to be underlined that our geometrical model using only 15 parameters correctly predicts all the size distributions.

One can now briefly compare the model proposed in this paper with other asymmetric models of the bronchial tree found in the literature. Two classical asymmetric models of the human bronchial tree were developed by Horsfield et al. (6). First, one has to note that both these models require more than one hundred parameters. From this point of view, Horsfield's models are more anatomical models as compared to the model proposed here which should be considered as a simplified mathematical model. In particular, the model that we propose takes advantage of the quasi self-similarity in the intermediate bronchial tree (23). This reduces drastically the number of parameters of the model.

Kitaoka et al. have also developed an asymmetric model of the tracheobronchial tree (10). It essentially consists in a set of algorithmic rules linked to anatomical and physiological considerations that allow to construct a 3D space-filling model. The airway sizes and their distributions thus depend on the 3D embedding. Note that in Kitaoka's model, the flow rate is used as a design parameter and linked to the airway diameter. In consequence, assuming identical flow rates in all terminal airways leads to the same cutoff condition that the one used in our model. To our knowledge, Kitaoka's model has not been used to describe oxygenation times and does not include the systematic asymmetry that we have implemented.

Other models (20,27) are also based on asymmetric branching but most of them consist on statistical measurements of anatomical data rather than the small set of parameters and rules used in this work.

Ventilation performances

In theory, if all acini are ventilated, the volume of oxygenated fresh air delivered to the acini is equal to the tidal volume (TV=0.5 L) minus the sum of the volume of the oropharyngeal and laryngeal cavity (ETV=106 mL) and the dead space volume

(DSV=150 mL), thus TV-ETV-DSV=0.24 L. Using equation (7) and our geometrical model, one can compute the amount of fresh air delivered to the acini. The value that we obtained is about 0.25 L, a result very close to the expected value.

Fig. 4.A presents the distribution of the oxygenation times. This distribution is spread, the computed transit times ranging from 0.39 s to 0.97 s. As a consequence, the oxygenation times range from 0.63 s to 1.21 s with a mean value equal to 1.0 s and a standard deviation of 0.07 s.

All acini receive fresh air since all transit times are smaller than 1.6 s. Yet, they do not receive the same quantity of fresh air. Fig. 4.B presents the distribution of the volume of fresh air delivered in each acinus. Note that the distribution of oxygenation times in the acini may contribute to distribute in time the oxygen supply to the blood during the breathing cycle. Note also that if the perfusion is not perfectly matched to the oxygen ventilation, the pulmonary shunt then could be a consequence of the large transit time to the exchange units: blood perfusion might be normal but ventilation fails to supply the perfused region for a sufficient duration.

Note that the same type of distribution of inspired external gas (like hyperpolarized gas) would necessarily induce an “inherent noise” in NMR imaging of the lung. To our knowledge, this effect which is a necessary consequence of the asymmetric nature of the tracheobronchial tree has never been considered.

Also, our study shows that the inhalation of toxic gases has to produce heterogeneous damages of the lung structure. So it could help to better define some respiratory rules in case of such a toxic inhalation.

Now, consider the distribution of the flow rate between different bronchia at the same generation. Because of the very large dispersion of the number of acini fed by these various bronchia, the flow rates might be distributed in a strongly heterogeneous

manner. This is an essential difference between symmetric and asymmetric trees. In the case of an asymmetric infinite tree, this could lead to a multifractal distribution (26). Such a pre-multifractal behavior can be observed in Fig. 5 which presents a 2D representation of the distribution of volumes of fresh air delivered at a given generation (in the figure, generation 12). This 2D representation is based on the *Mandelbrot tree* representation (12).

Randomization and robustness

The model presented above builds a unique deterministic tree. In order to account for the inherent physiological variability (resulting for instance from the biological growth process (8)), we have introduced two types of randomization procedure of the airway sizes. This has been achieved by implementing Gaussian randomizations of the diameter ratios. For the first model of randomization, we assume that at each branching, the deterministic values of the diameter ratios are modified according to:

$$\begin{aligned} h_{\min} &= h_{0,\min} + \sigma\, X(0,1) \\ h_{\max} &= h_{0,\max} + \sigma\, Y(0,1) \end{aligned} \qquad (8)$$

X and *Y* are independent Gaussian random variables centered on 0 and of standard deviation 1. σ is the standard deviation of both h_{min} and h_{max}.

In the second model of randomization, we assume that at each branching, h_{min} and h_{max} are correlated random variables such that:

$$\begin{aligned} h_{\min} &= h_{0,\min} + \sigma\, X(0,1) \\ h_{\max}^3 + h_{\min}^3 &= h_{0,\max}^3 + h_{0,\min}^3 \end{aligned} \qquad (9)$$

X is a Gaussian random variable centered on 0 and of standard deviation 1. Due to the second relation in Eq. (9), the total volume of the daughter branches is conserved even when their sizes are randomized.

In both models, the mean values $h_{0,min}$ and $h_{0,max}$ of these random variables correspond to the values given in Table 1. Moreover, diameter ratios of different bifurcations are assumed to be independent random variables. These Gaussian variations of the diameter ratios thus slightly randomize all diameters and lengths. In the latter case, the diameter ratios h_{min} and h_{max} of the same bifurcation are anti-correlated. This means that if, for instance, the randomized ratio h_{max} is larger than its mean value $h_{0,max}$, then h_{min} is smaller than its mean value $h_{0,min}$. In other words, if one daughter branch is larger than expected then the other daughter branch will be smaller.

As observed in Majumdar et al. (14), the airways of the first generations are less subject to physiological variability and are essentially determined by the anatomy. This specificity of the 4 first diameter ratios (generations 0-4) led us to randomize only the intermediate tree (above generation 4). In all two cases of randomizations, σ is chosen equal to 0.10 which corresponds to the standard deviation deduced from Raabe's data (14).

Fig. 6.A presents the measured distributions of generations of airways of diameter 2 mm and of airways giving rise to daughter branches of diameter smaller than 0.7 mm (31,6).

Fig. 6.B presents the computed distributions for the first type of randomization, when h_{min} and h_{max} are independent random variables. Clearly, the histograms do not fit the anatomical measurements. Also, the maximum generation number of the tree is much larger than 23 since the number of airways of diameter 2 mm at generation 23 is significant, contrary to the measurements in which they do not exist. This can be understood with a simple argument: the stochastic randomization can lead to large

values of both diameter ratios at several successive bifurcations. Consequently, a significant fraction of the airways downstream of these bifurcations would be large, leading to a drastic increase of the generation number of the terminal bronchioles.

Fig. 6.C presents the computed distributions for the second type of randomization, when h_{max} and h_{min} are anti-correlated random variables. The distributions are now closer to the measurements. One however observes that in the case of the Weibel's distribution (left column), the average generation number is larger than the measured one. This can be explained as previously by a different casting technique (7). This seems to prove that the anti-correlation of both diameter ratios is a key ingredient to reproduce the spread of the airway sizes in the tree.

The results described in Fig. 6 indicate that the system structure is sensitive to the type of randomizations of the diameter ratios. In particular, independent diameter ratios at each bifurcation may give rise to a large sub-tree, a situation that is not observed in the pulmonary anatomy. On the other hand, assuming anti-correlated diameter ratios has several consequences: first, the Hess-Murray law is almost verified at each bifurcation ($h_{\max}^3 + h_{\min}^3 = 0.87^3 + 0.67^3 \approx 0.96$). Second, the distributions of airway sizes appear to be identical at all generations for both deterministic (Fig. 1) and randomized trees (Fig. 6.C). In other words, the systematic asymmetry found in the intermediate tree induces a spreading of the airway sizes at every generation which somehow "hides" any additional randomization of the geometry. Finally, the ventilation performances which are determined by the airway size distribution would not be affected by the randomization of Fig. 6.C. In that sense, the systematic branching asymmetry provides a robustness of the ventilation against

the physiological variability which can be interpreted as a form of “structural protection”.

Application to the tracheobronchial tree of the rat

We now show that the method used for the human lung can be applied to the tracheobronchial tree of the Long-Evans rat. As for the human adult, the tree of a healthy adult rat spreads out from the trachea (generation 0) to the terminal airways located on average at generation 15 (34). The geometrical model for the rat is also built using data computed by Majumdar et al. (14) from measurements of Raabe et al. (22). Here also, the scaling is specific in the first generations due to anatomical constraints (13). A systematic self-similarity is assumed for generations larger than 4. Table 2 summarizes our model of the tree of a healthy adult Long-Evans rat weighting in average 320 g.

As in the human case, the tree ends at a given airway diameter: the corresponding measured average diameter of the terminal bronchioles is 0.20 mm (24,38). The length and radius of the trachea of a healthy adult rat are respectively taken equal to 34 mm and 1.7 mm (22), the tidal volume equal to 2 mL (2,36) and the average inspiration time equal to 0.2 s (2,36). The volume of the nasopharyngeal and laryngeal cavity is estimated to 0.31 mL (19,29): the time spent in this cavity is then equal to 0.03 s.

In this model, we first assume no randomization of the diameter ratios. The terminal bronchioles range from generation 6 to 23 with an average value around 13-14. The measurements show that the terminal bronchioles range from 8 to 25 with an average generation of 15 according to Weibel et al. (34). Our model leads to a number of acini close to 2800, a value comparable to the estimation of Yeh et al. (38) namely 2487 acini, whereas Rodriguez et al. (24) estimated this number to 2012. The

calculated DSV is about 1.23 mL, close to the measured DSV for healthy adult Long-Evans rats weighting approximately 300 g: 1.10 mL in (38) and 1.15 mL in (16). Note here that the rat airway structure is subject to strong anatomical variability and that several casts would be necessary to have an average estimation of the DSV as reported by Menache et al. (16).

The model reproduces anatomical data from Raabe (22) based on manual airway measurements, from Sera et al. (28) based on 3D data analysis process without fixation and dehydration of lung tissue, and from Lee et al. (13) based on 3D data analysis process (Fig. 7). Note here that above generation 10, the average airway diameter computed by our model and plotted in Fig. 7 seems to vary with a small periodicity of 3. As in Fig. 1D, this is again a discretization effect due to the use of exact diameter ratios and exact terminal cutoff. This effect can be cancelled by a small randomization of the diameter ratios. The model also reproduces the anatomical distribution of the airway sizes of a given generation (referred to the measurements of Raabe et al., results not shown).

The ventilation properties of the rat tree have also been computed. The transit times are found to range from 0.06 s to 0.19 s. As a consequence, the oxygenation times spread from 0 s to 0.11 s. Almost all the acini receive fresh air (98.5%). The total volume of fresh air delivered to the acini is estimated to 0.54 mL, close to the expected value of 0.5 mL assuming that all the acini receive fresh air.

As for Fig. 6.C of the human case, anti-correlated randomizations of the diameter ratios have been introduced. Again, the airway size distributions and the ventilation performances are observed to be robust against this anatomical variability.

Conclusions

In summary, we propose a geometrical model for the tracheobronchial tree that relies on three key ingredients. First, a specific scaling of the upper bronchial tree based on the anatomy. Second, a systematic branching asymmetry that spreads the distributions of airway sizes in the lung according to the measured distributions. This asymmetry is achieved around an average value of the diameter ratio close to 0.79 that ensures a small hydrodynamic resistance of the airways (15). Third, terminal bronchioles end at a given value of the diameter, which leads to a tree of variable depth depending on the pathway. When the diameter ratios are randomized, it is shown that a direct anti-correlation between daughter sizes of the same parent branch is still needed in order to reproduce the measured distributions. The principle used here is then to substitute a noisy symmetric tree structure, as for instance the Weibel description, by a deterministic but asymmetric structure. The same method applied to the tracheobronchial tree of the Long-Evans rat permits to build a similar geometrical model that is also in good agreement with the anatomical and functional ventilation characteristics of the rat.

This model appears to be simple and parsimonious. Therefore it is particularly adapted to analytical or numerical studies such as the computation of air flow or particle deposition. For instance, by adding airway compliance laws, this model allows to compute the dynamical behavior of the bronchial tree during the breathing cycle (3). Embedding this model in 3D would also permit to reproduce and analyze images of ventilation obtained by NMR of hyperpolarized gas. By modeling alterations of the geometry in specific regions or generations of the airway system, this model could help to understand the relationship between geometrical or anatomical characteristics of the tree and pathologies such as chronic obstructive

pulmonary disease or asthma. Finally, one can note that the concept of asymmetric branching leads to the idea that pathological perturbations of bronchial properties would necessarily lead to heterogeneous consequences.

References

1. **Beech DJ, Sibbons PD, Howard CV, Van Velzen D.** Terminal bronchiolar duct ending number does not increase post-natally in normal infants. *Early Hum Dev* 59: 193-200, 2000.

2. **Correa FCF, Ciminelli PB, Falcao H, Alcantara BJC, Contador RS, Medeiros AS, Zin WA, Rocco PRM.** Respiratory mechanics and lung histology in normal rats anesthetized with sevoflurane. *J Appl Physiol* 91: 803-810, 2001.

3. **Florens M, Sapoval B, Filoche M.** The optimal branching asymmetry of a bidirectional distribution tree. *Comp Phys Commun.* doi:10.1016/j.cpc.2010.11.008.

4. **Hess WR.** *Das Prinzip des kleinsten Kraftverbrauches im Dienste hämodynamisher Forschung Archiv für Anatomie und Physiologie,* edited by Physiologische Abteilung, 1914.

5. **Horsfield K, Cumming G.** Morphology of the bronchial tree in man. *J Appl Physiol* 24: 373-383, 1968.

6. **Horsfield K, Dart G, Olson DE, Filley GF, Cumming G.** Models of the human bronchial tree. *J Appl Physiol* 31: 207-217, 1971.

7. **Hughes JMB, Hoppin FG Jr, Mead J.** Effect of lung inflation on bronchial length and diameter in excised lungs. *J Appl Physiol* 32: 25-35, 1972.

8. **Hutchins GM, Haupt HM, Moore GW.** A proposed mechanism for the early development of the human tracheobronchial tree. *Anat Rec* 201: 635-640, 1981.

9. **Kitaoka H, Suki B.** Branching design of the bronchial tree based on a diameter-flow relationship. *J Appl Physiol* 82: 968-976, 1997.

10. **Kitaoka H, Takaki R, Suki B.** A three-dimensional model of the human airway tree. *J Appl Physiol* 87: 2207-2217, 1999.

11. **Lambert RK, Wilson TA, Hyatt RE, Rodarte JR.** A computational model for expiratory flow. *J Appl Physiol* 52: 44-56, 1982.

12. **Lauwerier, H.** *Fractals: Endlessly Repeated Geometric Figures*, edited by Princeton Univ. Press: Princeton, 1991.

13. **Lee D, Fanucchi MV, Plopper CG, Fung J, Wexler AS.** Pulmonary architecture in the conducting regions of six rats. *Anat Rec* 291: 916-926, 2008.

14. **Majumdar A, Alencar AM, Buldyrev SV, Hantos Z, Lutchen KR, Stanley HE, Suki B.** Relating Airway Diameter Distributions to Regular Branching Asymmetry in the Lung. *Phys Rev Lett* 95: 168101, 2005.

15. **Mauroy B, Filoche M, Weibel ER, Sapoval B.** An optimal bronchial tree may be dangerous. *Nature* 427: 633-636, 2004.

16. **Menache MG, Patra AL, Miller FJ.** Airway structure variability in the Long-Evans rat lung. *Neurosci Biobehav Rev* 15: 63-69, 1991.

17. **Murray CD.** The physiological principle of minimum work. The vascular system and the cost of blood. *Proc Natl Acad Sci U.S.A* 12: 207-214, 1926.

18. **Patra AL.** Comparative anatomy of mammalian respiratory tracts: the nasopharyngeal region and the tracheobronchial region. *J Toxicol Environ Health* 17: 163-174, 1986.

19. **Patra AL, Ménache MG, Shaka NB, Gooya A.** A morphometric study of nasal-pharyngeal growth for particle deposition in the rat. *Am Ind Hyg Assos J* 48: 556-562, 1987.

20. **Phillips CG, Kaye SR.** Diameter-based analysis of the branching geometry of four mammalian bronchial trees. *Resp Physiol* 102: 303-316, 1995.

21. **Phillips CG, Kaye SR.** On the asymmetry of bifurcations in the bronchial tree. *Resp Physiol* 107: 85-98, 1997.

22. **Raabe OG, Yeh HC, Schum GM, Phalen RF.** Tracheobronchial Geometry: Human, Dog, Rat, Hamster. *Tech Rep Publ* No. LF-53, 1976.

23. **Restrepo JG, Ott E, Hunt BR.** Scale dependence of branching in arterial and bronchial trees. *Phys Rev Lett* 96: 128101, 2006.

24. **Rodriguez M, Bur S, Favre A, Weibel ER.** Pulmonary acinus: geometry and morphometry of the peripheral airway system in rat and rabbit. *Am J Anat* 180: 143-155, 1987.

25. **Sandeau J, Katz I, Fodil R, Louis B, Apiou-Sbirlea G, Caillibotte G, Isabey D.** CFD simulation of particle deposition in a reconstructed human oral extrathoracic airway for air and helium–oxygen mixtures. *J Aero Sci* 41: 281-294, 2010.

26. **Sapoval B.** *Universalités et Fractales*, edited by Flammarion: Paris, 1997.

27. **Schmidt A, Zidowitz S, Kriete A, Denhard T, Krass S, Peitgen HO.** A digital reference model of the human bronchial tree. *Comp Med Imaging Graphics* 28: 203-211, 2004.

28. **Sera T, Fujioka H, Yokota H, Makinouchi A, Himeno R, Schroter RC, Tanishita K.** Three-dimensional visualization and morphometry of small airways from microfocal X-ray computed tomography. *J Biomech* 36: 1587-1594, 2003.

29. **Schreider JP, Raabe OG.** Anatomy of the nasal-pharyngeal airway of experimental animals. *Anat Rec* 200: 195-205, 1981.

30. **Tawhai MH, Hunter P, Tschirren J, Reinhardt J, McLennan G, Hoffman EA.** CT-based geometry analysis and finite element models of the human and ovine bronchial tree. *J Appl Physiol* 97: 2310-2321, 2004.

31. **Weibel ER.** *Morphometry of the human lung,* edited by Springer Verlag and Academic Press: Berlin and New york, 1963.

32. **Weibel ER.** *The Pathway for Oxygen, Structure and Function in the Mammalian Respiratory System*, edited by Harvard University Press: Harvard, 1984.

33. **Weibel ER.** Design of airways and blood vessels considered as branching trees. In: *The Lung: Scientific Foundations.* Crystal RG, West JB, Weibel ER, Barnes PJ: Lippincott-Raven Publishers, Philadelphia, 1997, chapt. 74, p. 1061-1071.

34. **Weibel ER, Sapoval B, Filoche M.** Design of peripheral airways for efficient gas exchange. *Resp Physiol Neurobiol* 148: 3-21, 2005.

35. **West JB.** *Respiratory Physiology. The Essentials. 8th Edition*, edited by Lippincott-Raven Publishers: Philadelphia, 2008.

36. **Whitehead GS, Kimmel EC, Reboulet JE, Still KR.** Pulmonary function in normal rats. *Naval health research center detachment* Report No Toxdet 99-5, 1999.

37. **Yeh HC, Phalen RF, Raabe OG.** Factors influencing the deposition of inhaled particles. *Environmental Health Perspectives* 15: 147-156, 1976.

38. **Yeh HC, Schum GM, Duggan MT.** Anatomic models of the tracheobronchial and pulmonary regions of the rat. *Anat Rec* 195: 483-492, 1979.

Figure legends

Figure 1: A and C: Distributions of generations for airways of diameter 2 mm (A: Weibel measurements (histogram) and fit (line) (adapted from 31); C: our model). B and D: Distributions of the number of divisions from the trachea down to the first branch giving rise to daughter branches of diameter smaller than 0.7 mm (B: Horsfield measurements (line) and model (line in bold) (adapted from 6); D: our model).

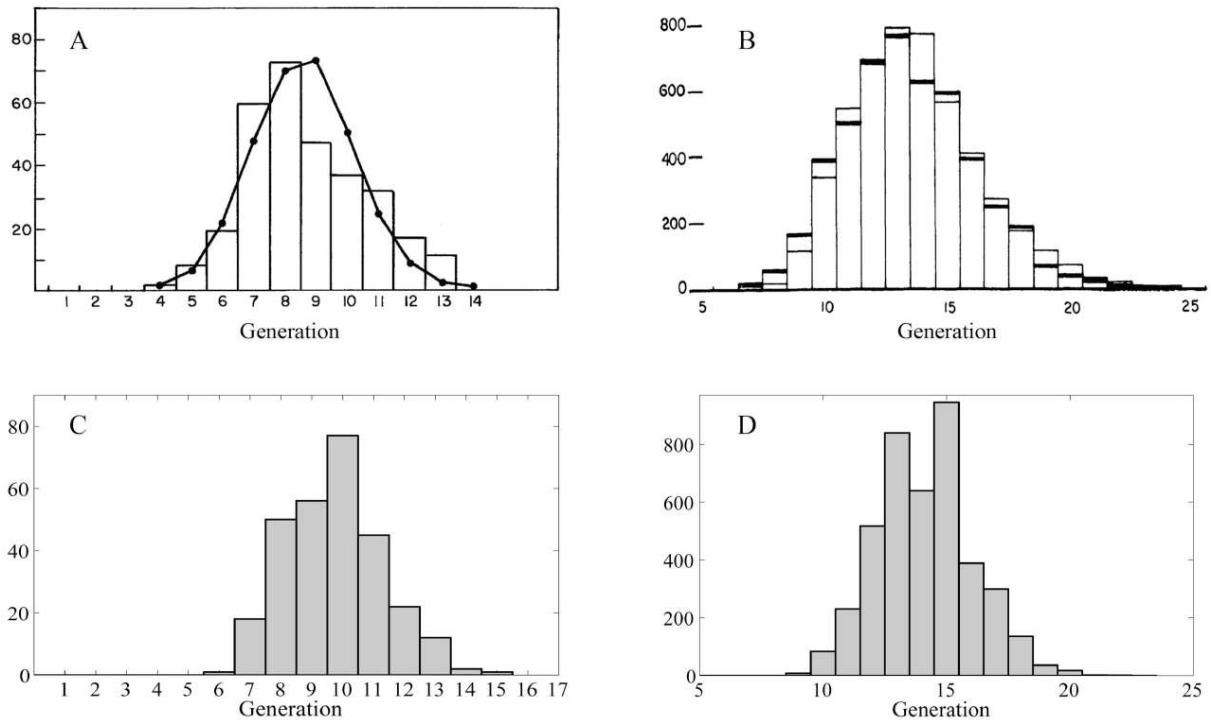

Figure 2: The description of the asymmetry: the major (resp. minor) daughter airway corresponds to the daughter airway with larger (resp. smaller) diameter D_{max} (resp. D_{min}). The diameter ratios $h_{0,max}$ and $h_{0,min}$ are defined by the ratio of the daughter diameter over the parent diameter D_0 for the major and the minor airway.

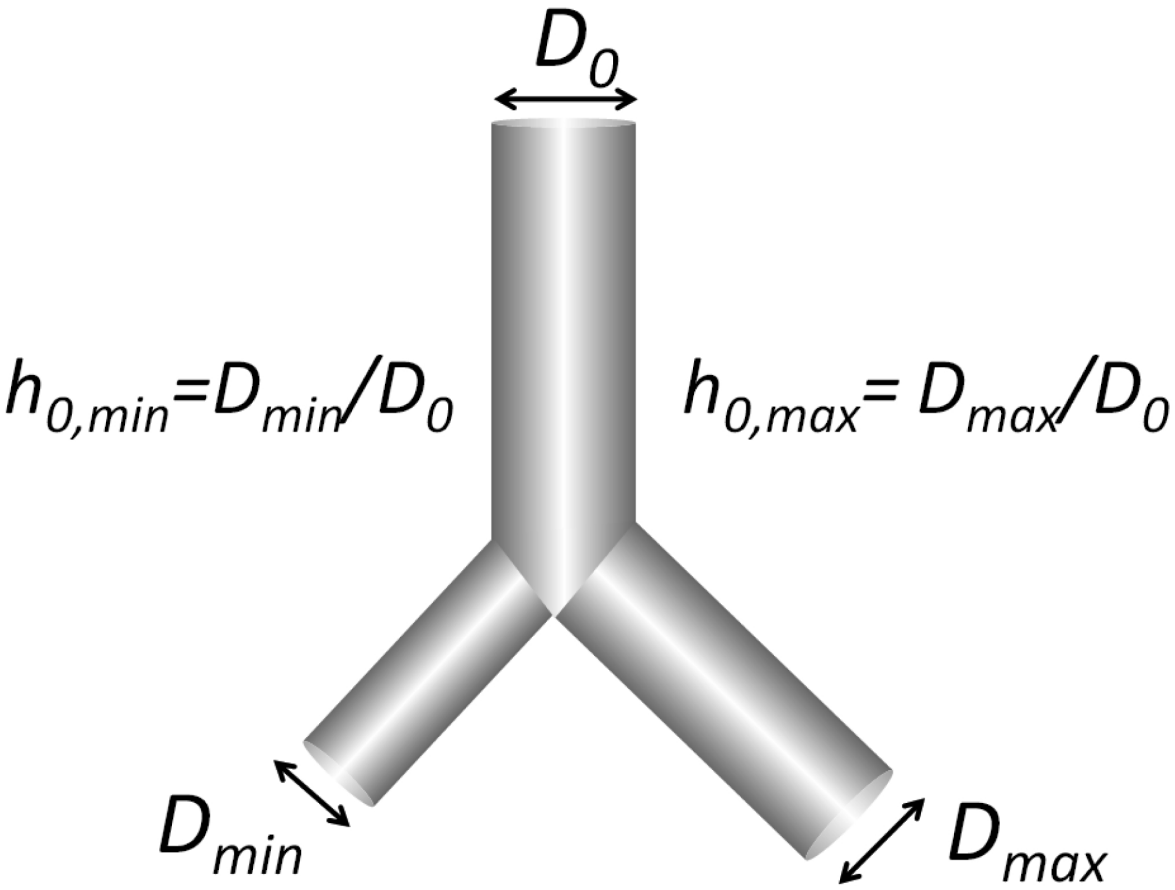

Figure 3: Distribution of airway diameters in generations 1 to 10. The generation numbers are plotted on top right of each panel. The histograms on the left are the distributions measured by Weibel on the cast (31), the lines on the left represent the Weibel's fit. The filled bars are the airway classes which were completely sampled and the open bars are the airway classes which were partially sampled. The figures on the right were computed with our model.

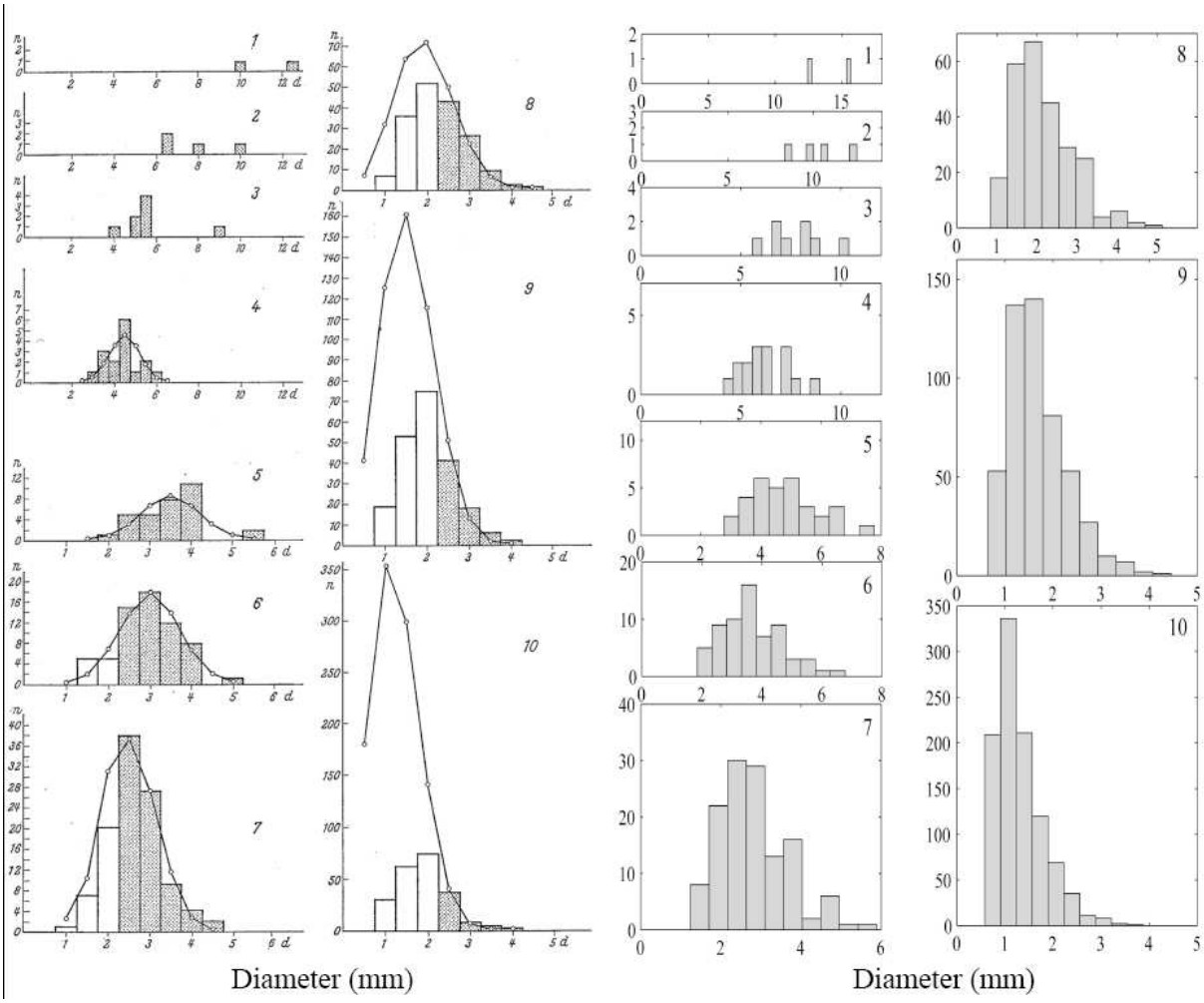

Figure 4: A: Distribution of oxygenation times in the acini. B: Distribution of the volumes of fresh air delivered to each acinus.

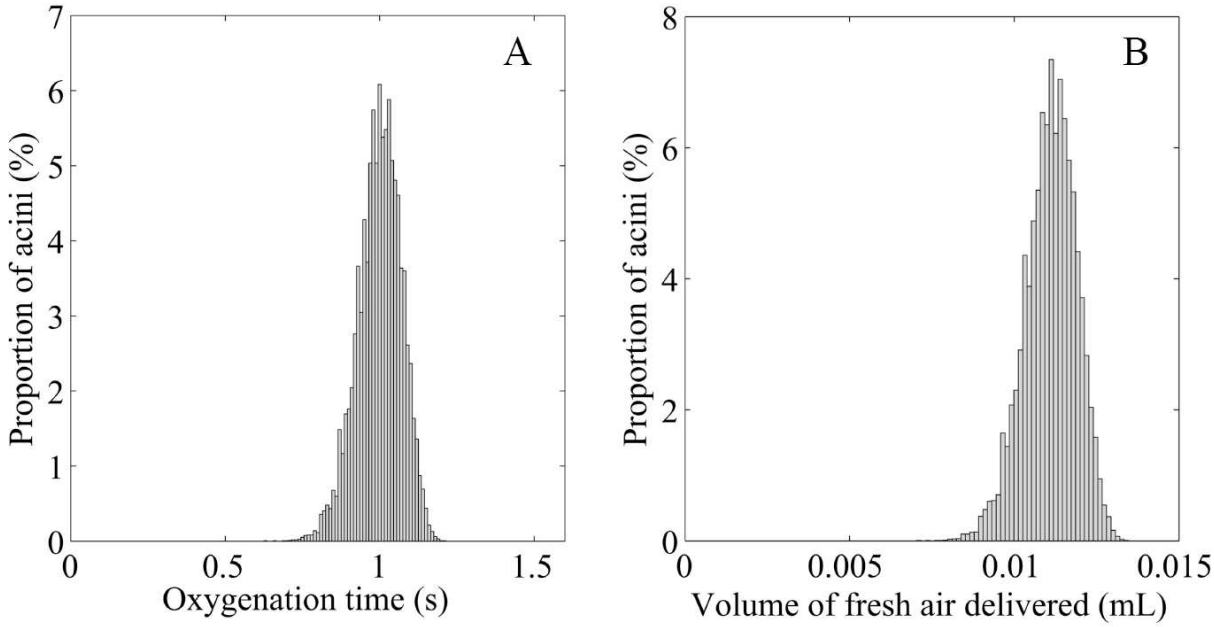

Figure 5: 2D representation of the distribution of volumes of fresh air crossing generation 12 in the proposed model. There are 2^{12} squares, each of which represents one airway at generation 12. The colors correspond to the logarithm of the distributed volume of fresh air expressed in milliliters. The black squares correspond to airways that are too small (D<0.5 mm) to belong to the tracheobronchial tree.

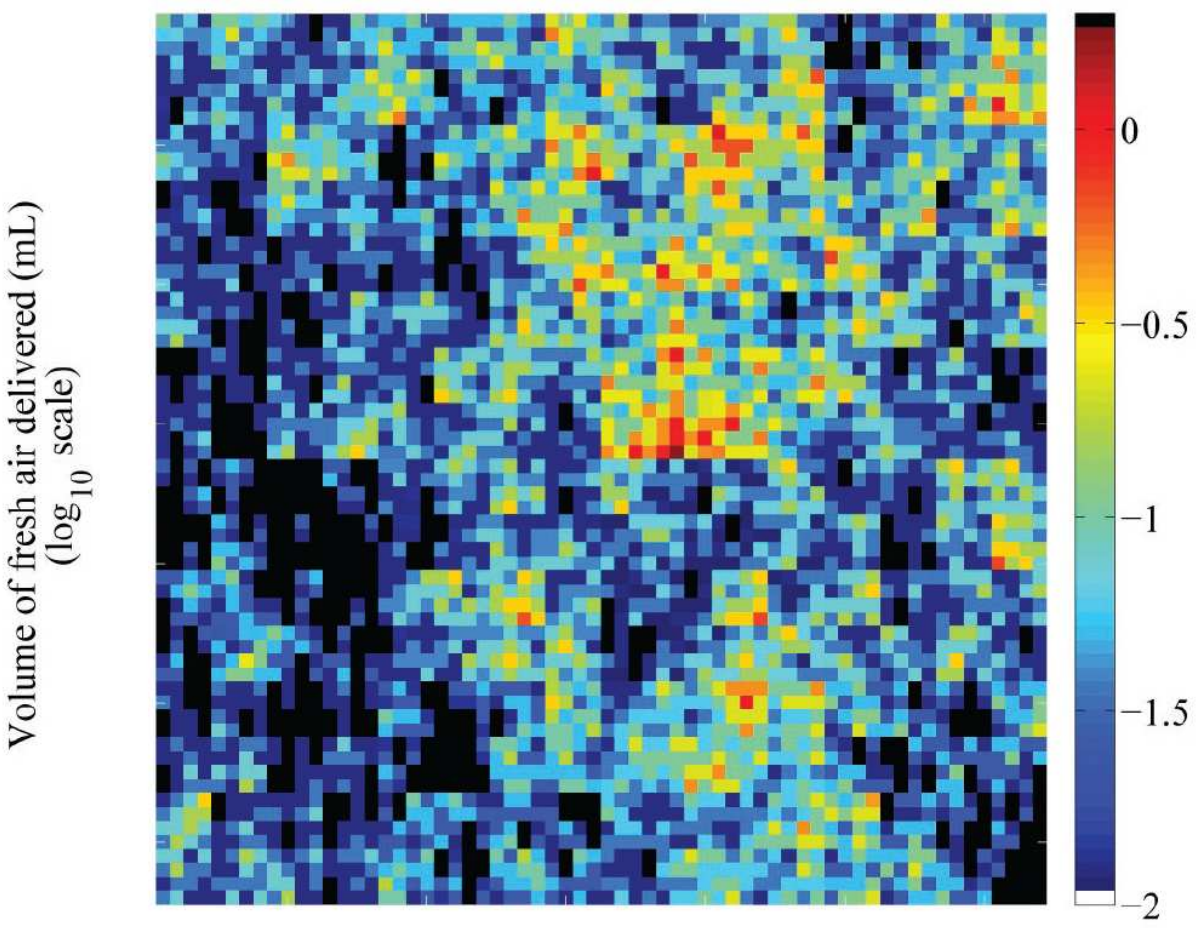

Figure 6: The figures on the left are the distributions of generations for airways of diameter 2 mm and the figures on the right the distributions of generations of the first branch giving rise to daughter branches of diameter smaller than 0.7 mm. A: Anatomical measurements (adapted from 31,6). B: Independent random diameter ratios above generation 4. C: Anti-correlated random diameter ratios above generation 4.

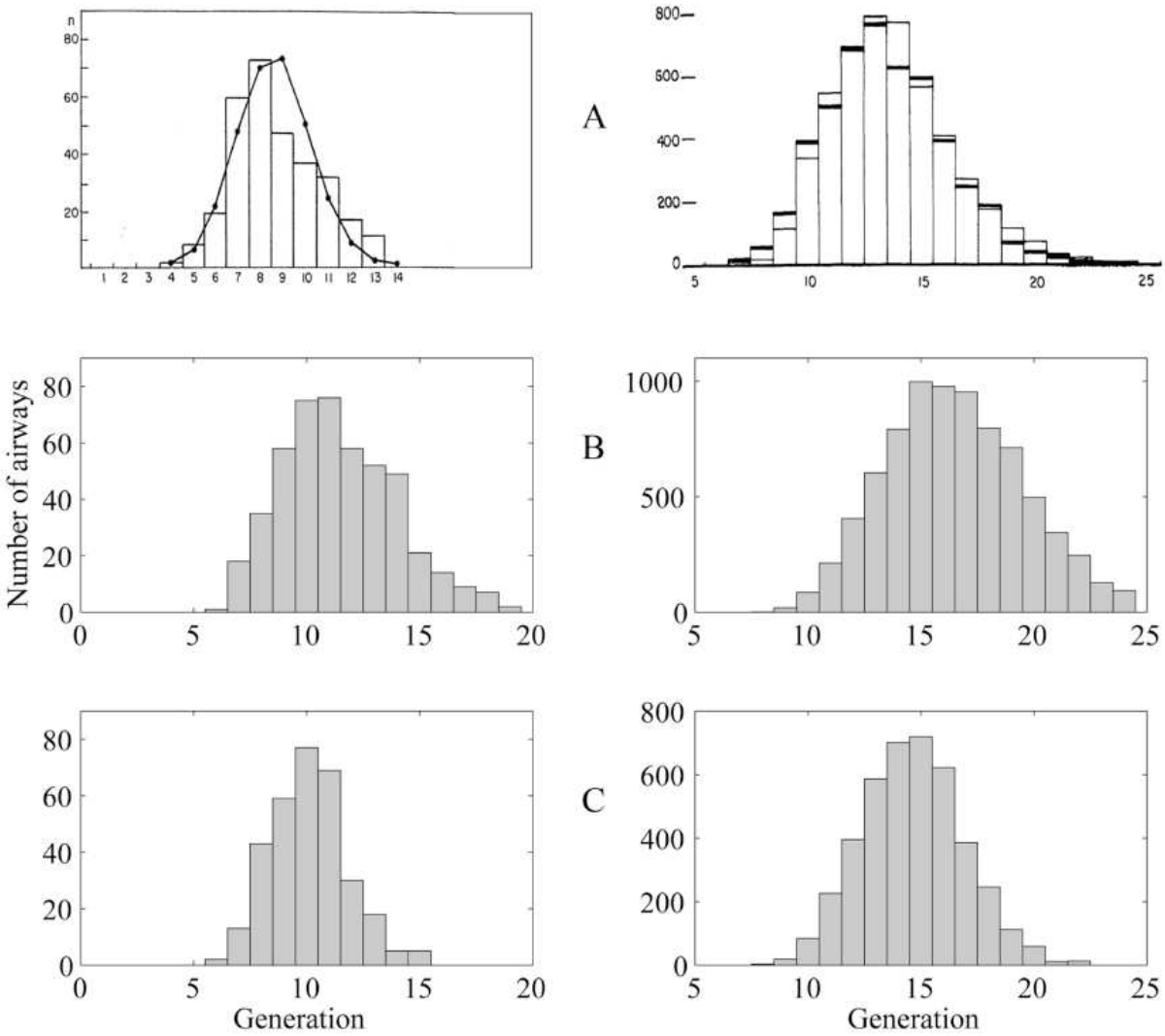

Figure 7: Plot of the average airway diameter as a function of the generation in the rat bronchial tree. Comparison between our model and various anatomical measurements from the literature (22,28,13).

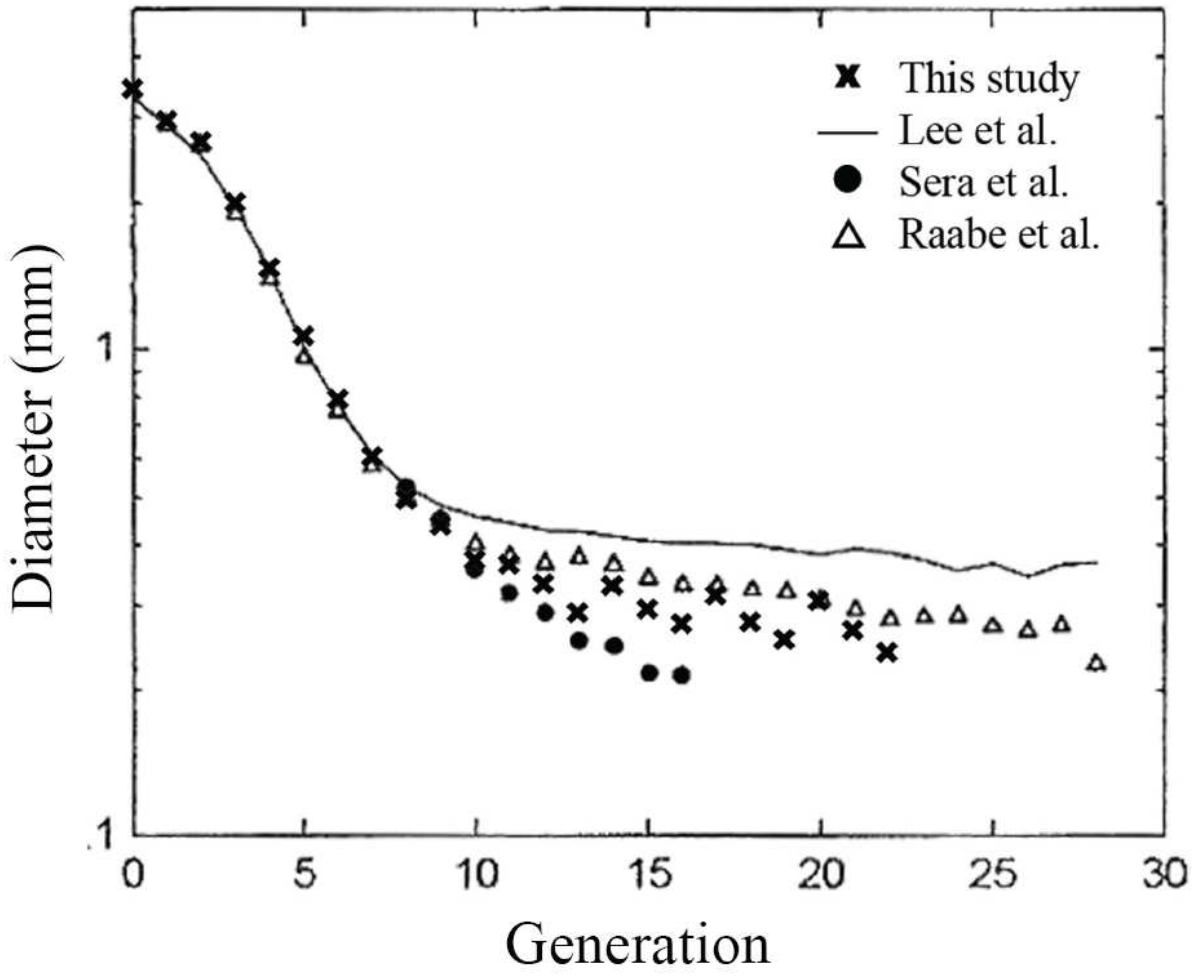

Table legends

Table 1. *Simplified asymmetrical model of the human tracheobronchial tree, derived from the analysis of (22,14).*

	Generation	Diameter ratio for the diameter D^*		Ratio $L^{\dagger}/D$
		$h_{0,max}$	$h_{0,min}$	
Specific geometry	1	0.87	0.69	3.07
	2	0.80	0.67	1.75
	3	0.83	0.67	1.43
	4	0.86	0.74	1.85
Self-similar intermediate tree	5-23	0.87	0.67	3.00

*: Airway diameter. †: Airway length.
Ending condition: D=0.5 mm

Table 2. *Simplified asymmetrical model of the rat tracheobronchial tree, derived from the analysis of (22,37,14).*

	Generation	Diameter ratio for the diameter D^*		Ratio $L^\dagger/D$
		$h_{0,max}$	$h_{0,min}$	
Specific geometry	1	0.89	0.83	2.81
	2	1.19	0.62	1.68
	3	0.90	0.60	1.07
	4	0.90	0.57	1.75
Self-similar intermediate tree	5-23	0.87	0.58	1.65

*: Airway diameter. †: Airway length.
Ending condition: D=0.2 mm